Catalysis Today 147S (2009) S138–S143

Contents lists available at ScienceDirect

Catalysis Today

journal homepage: www.elsevier.com/locate/cattod

Intensification of co-current gas–liquid reactors using structured catalytic packings: A multiscale approach

D. Vervloet [a,*], M.R. Kamali [b], J.J.J. Gillissen [b], J. Nijenhuis [a], H.E.A. van den Akker [b], F. Kapteijn [c], J.R. van Ommen [a]

[a] Product and Process Engineering, Delft University of Technology, Julianalaan 136, 2628 BL, Delft, The Netherlands
[b] Multiscale Physics Department, Delft University of Technology, Prins Bernhardlaan 6, 2628 BW, Delft, The Netherlands
[c] Catalysis Engineering, Delft University of Technology, Julianalaan 136, 2628 BL, Delft, The Netherlands

ARTICLE INFO

Keywords:
Multiphase reactor design
Tubular reactor
Structured packings
Heat transfer
Flow distribution

ABSTRACT

Cross-flow structured packings for tubular fixed bed reactors operated with co-current gas–liquid flow perform significantly better in terms of overall heat transfer than a randomly packed bed (glass beads), knitted wire packing, and Al-foam structure at a range of gas and liquid flow rates. This is mainly the result of radial directed convective transport of heat, realized by the channel structure of the cross-flow packings. A pseudo-homogeneous 2D (two-dimensional) plug flow model is found inadequate to quantify variations in overall heat transfer for experiments with different packing orientations and different gap sizes between the packing structure and the cooling wall, because it does not take directed convective transport of heat into account. Numerical simulations are performed to investigate in detail the fluid flow inside the packing. The geometry is defined as sheets separating layers of diagonal channels. For simplicity we assume no fluid exchange between different layers and we approximate the flow in the individual layers as 2D. The simulated velocity distribution inside the packing is highly inhomogeneous, showing regions of almost zero flow. These inhomogeneities in the flow are shown to depend on geometrical parameters, such as the packing width-to-height ratio and can have strong impact on reactor efficiency.

© 2009 Elsevier B.V. All rights reserved.

1. Introduction

Heterogeneous catalysis plays a key role in many processes in the chemical industry. Often the reactants and the products exist in different phases, which can cause inefficiencies because of poor reactant–catalyst contacting, e.g. bypassing, maldistribution, and incomplete wetting. The introduction of structure in reactors is essential to optimize the performance with respect to the phenomena and dynamics that govern at various scales in the reactor, ranging from molecular (catalyst) level to reactor scale [1]. It is expected that imposing structure on the reaction environment of three-phase tubular fixed bed reactors can lead to significant improvements in reactor performance [2]. The motivation for using structured geometries in tubular reactors is to control the fluid flow paths in the reaction environment, hereby (1) improving gas–liquid–solid contacting in order to maximally exploit catalytic performance, (2) establishing flow dynamics that minimize axial mixing in order to obtain narrow residence time distributions, and (3) maximizing mixing in the radial direction in order to improve heat transport from the reaction mixture to the wall. The latter one is particularly important for the reaction kinetics that strongly depend on temperature and concentration variations, such as the highly exothermal Fischer–Tropsch reaction [3,4]. Realizing uniform radial temperature and concentration profiles in a tubular fixed bed reactor can greatly improve the reactor performance [5]. Structured packings based on cross-flow geometries are a good candidate for securing these objectives, while preserving a relatively large surface area and low pressure drop [6]. Understanding the fluid dynamics of these systems is imperative for design purposes, such as mass/heat transfer rates, residence time distribution, fluid hold-up, and consequently conversion. In this paper we investigate the heat transfer characteristics and flow dynamics of structured packings based on a cross-flow geometry for co-current operated tubular fixed bed reactors.

1.1. Structured packings for tubular fixed bed reactors

Radial heat transfer in tubular reactors can be significantly improved through the introduction of a geometry that allows for cross-flow in the reaction environment. Cross-flow is convective flow of reactants that has a component perpendicular to the axial reactor direction, which improves the heat transfer by means of

* Corresponding author. Tel.: +31 15 278 4685.
E-mail address: d.vervloet@tudelft.nl (D. Vervloet).

0920-5861/$ – see front matter © 2009 Elsevier B.V. All rights reserved.
doi:10.1016/j.cattod.2009.07.015

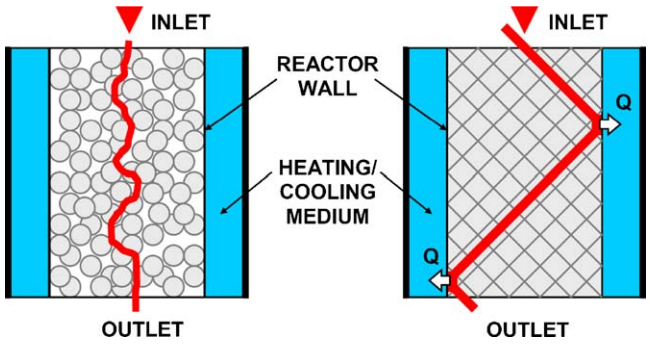

Fig. 1. Possible flow paths of reactants (co-current, top-down) through an axial cross-section of a randomly packed bed (left) and a cross-flow structured geometry (right).

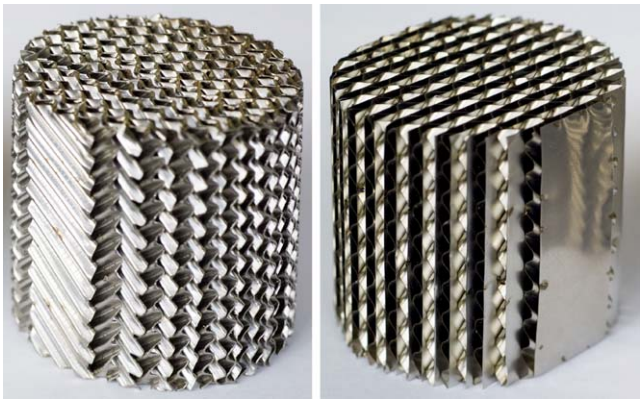

Fig. 4. Photos of the OCFS (left) and CCFS (right) packings.

radial convective transport in addition to the generally small radial conductive heat transport. This can be realized by choosing a geometry that consists of slanted channels. Fig. 1 shows a schematic view of a possible flow path in an axial cross-section of a randomly packed bed and a cross-flow structured geometry.

Depending on the type of cross-flow structure (CFS) mixing of the reactant flows from different channels can take place at various locations. Two types of CFS are distinguished: (1) the open CFS (OCFS) and (2) the closed CFS (CCFS). Examples of these types of structures are Katapak-MK and Mellapak, developed and manufactured by Sulzer [7]. An OCFS packing consists of a stack of corrugated plates with alternating angle configuration (e.g. 45° and −45°). The channels are formed by the corrugations in the sheets. In this case the reactants in the channels are allowed to mix with those of the channels from a neighboring plate at cross-sections and in the gap between the reactor wall and the packing structure (see Fig. 2). In a CCFS geometry mixing between the channels of two neighboring plates is prohibited, due to the presence of flat sheets between the corrugated sheets (see Fig. 2).

Evaluation of the mixing zones leads to the visualization of the possible flow paths in the OCFS and CCFS packings, which is depicted in Fig. 3. Three types of flow paths exist inside the OCFS packing: (a) flow through the center of the packing moving to the neighboring layer at each cross-section, (b) flow through the gap between the packing and the reactor wall, and (c) flow through the channels of the packing exiting the channel at the reactor wall and entering a new channel. For the CCFS packing flow type (a) is blocked by the flat sheets; hence only flow types (b) and (c) take place. The actual flow through the packings is a combination of all possible flows.

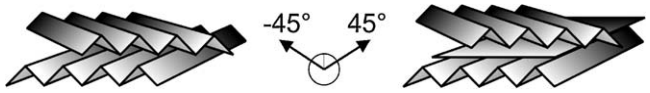

Fig. 2. Visualization of the OCFS (left) and CCFS (right) structures.

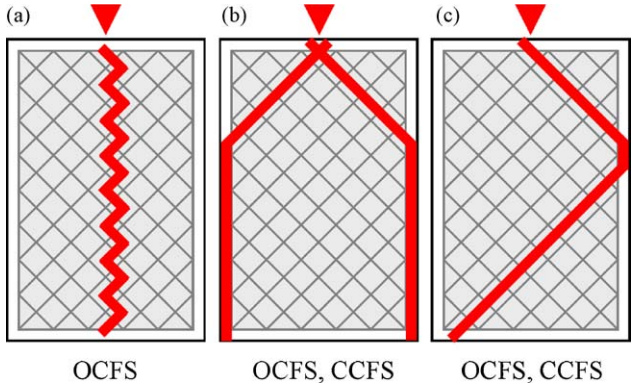

Fig. 3. Types of flow through an axial cross-section of the packing: (a) flow through the center of the packing moving to the neighboring layer at each cross-section, (b) flow through the gap between the packing and the reactor wall, and (c) flow through the channels of the packing exiting the channel at the reactor wall and entering a new channel.

Note that although the fluids follow a tortuous flow path, this does not automatically imply that plug flow conditions cannot exist. All tortuous flow paths through the packings are of the same length, and therefore plug flow conditions can exist. Deviations from plug flow may arise through either (1) bypassing of the flow through the gap or (2) uneven flow distribution through the channels. Photos of the constructed packings are given in Fig. 4.

1.2. Multiscale approach

We approach the challenges that are associated with the transport phenomena on different length-scales, i.e. the tubular scale (meso-scale) and the channel scale (micro-scale). The strengths of both numerical and experimental work are combined. Reactor operation and performance characteristics in a conceptual process design, i.e. the macro-scale, will not be addressed in this paper.

2. Meso-scale—Experimental

The meso-scale deals with phenomena that take place at length-scales ranging from the tube diameter to tube length. The results of heat transfer experiments at different gas and liquid velocities are shown for the OCFS and CCFS packings, compared to those of a randomly packed bed, an open foam packing, and a knitted wire packing.

In order to measure the overall heat transfer coefficient (U_{ov}) of the packings a custom built set-up is used to measure the gas and liquid temperatures at the entrance and exit of the tube. The temperature profiles at various axial locations in the tube are also monitored. Fig. 5 shows a schematic representation of the set-up. The column (5.0 cm Ø), which consists of an insulated precolumn (1.0 m long) and a cooling column (80 cm long), is loaded with a specific packing type. The function of the precolumn is to eliminate any possible entrance effects in the flow.

Gas (N_2) and liquid (isopar-M, an organic liquid with diesel-like properties) are heated to 65 °C and fed to the precolumn. When the mixture enters the cooling column, heat is transferred to the cooling liquid (water), cooling the mixture to approximately 30 °C, depending on the flow rates and the packing properties. Inside the tube the temperature profile is measured by arrays of seven thermocouples (type K) at various axial locations. The radial

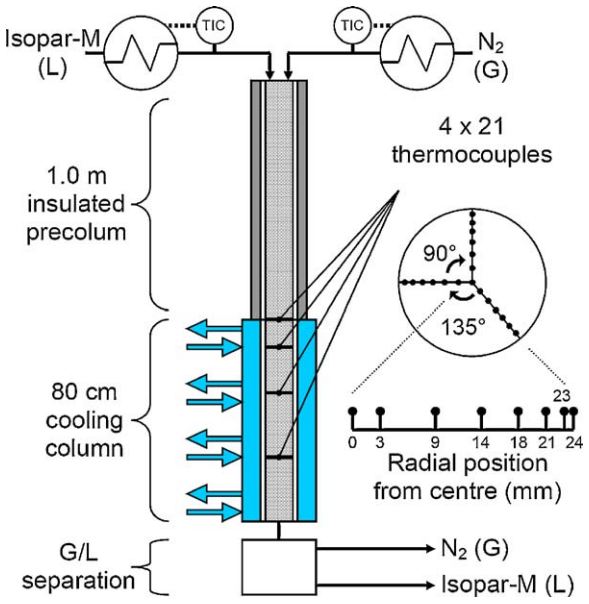

Fig. 5. Schematic representation of the set-up to measure the radial temperature profiles at various locations in the tube in three radial directions.

temperature profiles are measured in three different directions. Measurements were performed with different packings and different packing orientations at superficial liquid velocities ranging from 5 m/s to 22 m/s and superficial gas velocities ranging from 0.4 m/s to 2.6 m/s. Several packing properties are listed in Table 1: the porosity (ε), the hydraulic channel diameter (d_h), the specific surface per reactor volume (a_v), and the static contribution of the material to the radial effective thermal conductivity (λ_{static}).

The overall heat transfer coefficient, U_{ov}, is calculated using the logarithmic mean temperature difference of the middle section of the cooling column.

2.1. Results and discussion

The results for different packings operated at different superficial gas and liquid velocities are shown in Fig. 6, adapted from Pangarkar et al. [8]. In general the overall heat transfer increases

Table 1
Investigated packings and parameters.

Packing type	Material	ε	d_h (mm)	a_v (m^{-1})	λ_{static} ($W\,m^{-1}\,K^{-1}$)
Glass beads	Silica	0.4	0.9	2000	0.08
Knitted wire	Stainless steel	0.9	1.9	1930	1–3
Open foam	Aluminium	0.9	2.4	1900	20–25
OCFS	Stainless steel	0.84	1.8	1885	2–4
CCFS	Stainless steel	0.95	1.6	2400	1

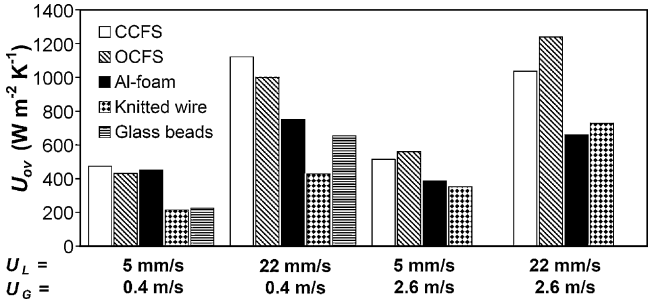

Fig. 6. Calculated overall heat transfer, U_{ov}, at various superficial gas and liquid velocities for different packings.

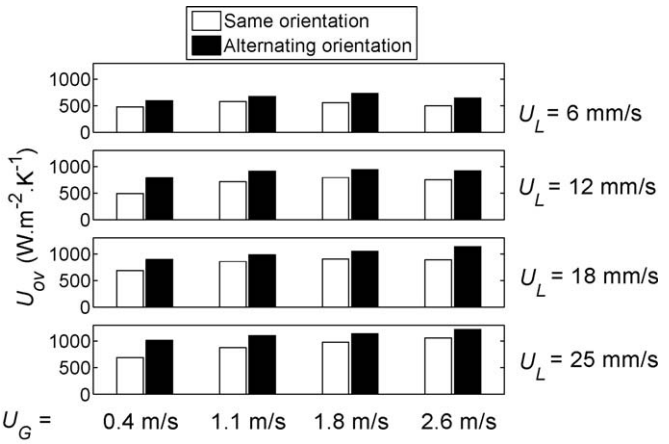

Fig. 7. Overall heat transfer coefficient, U_{ov}, for different OCFS packing orientations, i.e. same orientation and alternating orientation at different superficial gas and liquid velocities.

strongly with the liquid flow rate, and is only weakly dependent (OCFS, knitted wire) or independent (Al-foam, CCFS) on the gas flow rate. The CFS geometries are found to transfer up to 2.5 times more heat than other packings depending on the flow conditions. At the highest gas velocities the set-up could not be operated with the glass beads due to pressure drop limitations.

We conjecture from the observed increase in the overall heat transfer coefficient of the CFS packings that the promotion of radial heat transfer by means of directed convective transport plays an important role.

The effect of periodic redistribution of the flow inside a structured geometry due to stacking of elements can be seen in Fig. 7. In this figure the effect of the OCFS packing orientation in the stack, i.e. all packing elements in the same orientation or in alternating 90° rotated orientation, is presented in terms of overall heat transfer.

In all cases an alternated rotation of the packing elements yields a higher overall heat transfer coefficient by 15–60%. Similar results were obtained for the CCFS packing.

The effect of small variations in the gap size is shown in Fig. 8. Three categories of OCFS packings with different gap sizes have been studied: ~0.1 mm, ~0.3 mm, and ~0.5 mm.

The effect of the gap size on the overall heat transfer is not significant for low superficial gas velocities. At the largest superficial gas velocity the largest gap size is found to show a 37–54% higher overall heat transfer than that of the medium gap size. Also a narrow gap results in a better heat transfer. A general

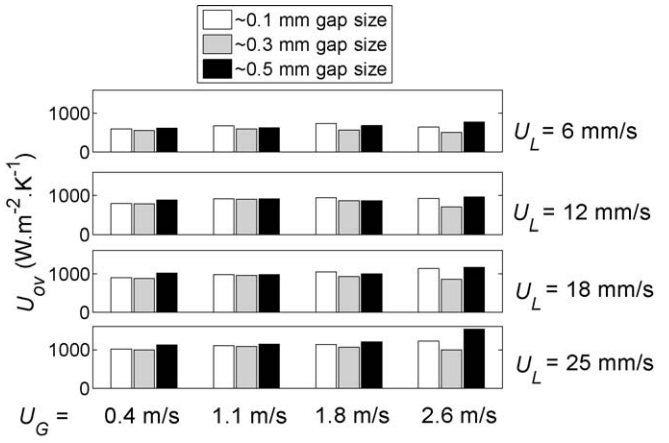

Fig. 8. Overall heat transfer coefficient, U_{ov}, for OCFS with different gap sizes: ~0.1 mm, ~0.3 mm, and ~0.5 mm operated at alternating packing orientation.

approach to quantify the effects of radial heat transport and wall heat transfer resistance is given by the two-dimensional pseudo-homogeneous plug flow model [9]. This model has also been applied in a similar study by Schildhauer et al. [10]. The curvature of temperature (T) over the axial (z) and radial (r) positions (Eq. (1)) of a tube (radius R) depends on the superficial velocities (u), specific heats (C_p, assumed constant), and densities (ρ, assumed constant) of the liquid (L) and gas (G), as well as the effective radial heat conductivity ($\lambda_{e,r}$, assumed constant and isotropic) and the wall heat transfer coefficient (α_w, assumed constant):

$$(u_L C_{p,L}\rho_L + u_G C_{p,G}\rho_G)\frac{\partial T}{\partial z} = \lambda_{e,r}\left[\frac{\partial^2 T}{\partial r^2} + \frac{1}{r}\frac{\partial T}{\partial r}\right] \quad (1)$$

With boundary conditions:

$$z = 0 : T = T_{in}; \quad r = 0 : \frac{\partial T}{\partial r} = 0; \quad r = R : -\lambda_{e,r}\frac{\partial T}{\partial r} = \alpha_w(T_{r=R} - T_w)$$

Furthermore, it is assumed that all phases (G, L, S) at any one point in the reactor are at the same temperature and that the gas- and liquid phases are in the plug flow regime. Key parameters $\lambda_{e,r}$ and α_w are determined by the packing structure and fluid flow properties. These are estimated by fitting Eq. (1) on the measured temperature profile, averaged for all three radial directions at every axial position in the tube. Since the cross-flow structures are not isotropic, i.e. the flow- and heat transfer properties are not the same in all radial directions, the significance of this model for CFS packings is doubtful. It was not attempted to separate the effective radial heat transfer coefficient for the different radial directions. In Fig. 9 the normalized radial temperature profile of an arbitrarily chosen experiment is depicted, as well as the resulting fit on Eq. (1).

Clearly, the (parabolic) partial differential equation does not give a representative description of the temperature profile inside the reactor loaded with OCFS packings. The Kolmogorov–Smirnov test also rejects the hypothesis that the residuals are normally distributed at a 95% confidence level. A similar result was found for the CCFS packings. CFS geometries show an increased heat transfer performance, which is not captured by the applied model. This indicates that the radial transport of heat does not follow a random path, and that directed convective transport of heat is a major contributor of the heat transport mechanism. Currently, we are developing such a model that takes directed convective transport of heat into account. A good understanding of the fluid flow is crucial to progress in this direction. For this purpose we use numerical tools.

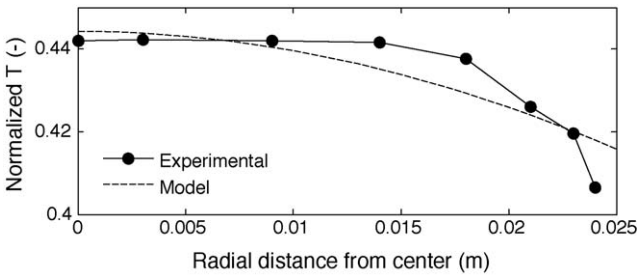

Fig. 9. Normalized radial temperature profile, $(T - T_c)/(T_{in} - T_c)$, of a heat transfer experiment with OCFS packings (z = 35 cm from inlet, U_L = 18 mm/s, U_G = 1.5 m/s) and fitted model.

3. Micro-scale—numerical approach

We use the Lattice Boltzmann (LB) method to numerically simulate the fluid flow inside the packing. The LB scheme used is based on the single relaxation time BGK (Bhatnagar–Gross–Krook) approximation [12], defined on the D2Q9 (two-dimensional, nine velocity components) lattice structure [11]. In the simulations, all relevant length-scales are resolved, from the packing geometry down to the individual channels.

The motivation for using the LB method for this particular problem is threefold. First, with the help of the LB method the complex geometry in the structured packing can be handled easily. Second, implementing parallel codes is straight forward, which is desirable for the highly demanding calculations in structured packings. Third, LB can simply handle the variety of mesoscopic forces and multi-physics involved in the type of processes in which structured packings are applied (such as Fischer–Tropsch synthesis) [11].

3.1. Problem description

We study single-phase, gravity driven flow through the CCFS packing. This packing consists of layers, which are composed of diagonal channels. The layers are separated by flat sheets, which inhibit fluid mixing between the different layers. Therefore we believe that the flow in these layers are independent and can be approximated as 2D. We have simulated the flow inside four different layers. Fig. 10b and Table 2 show the investigated 2D domains and the geometrical parameters used in the simulations.

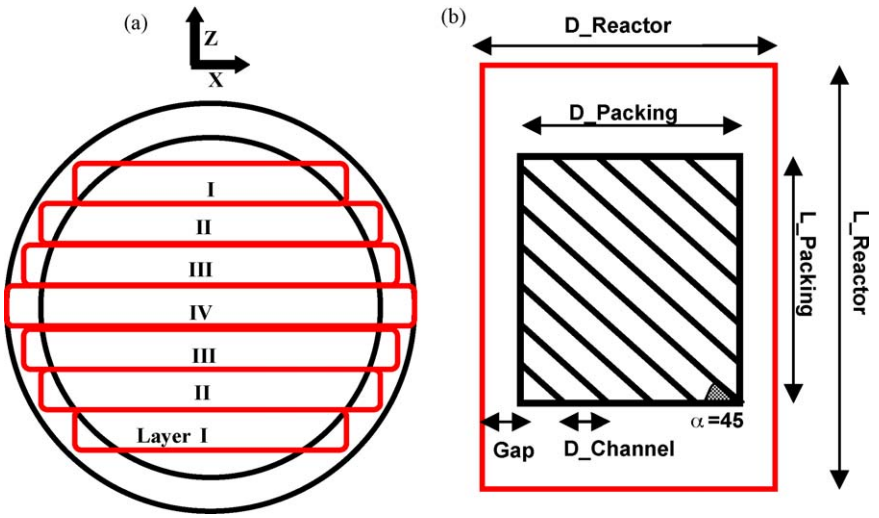

Fig. 10. (a) CCFS packing from top and (b) 2D layer of CCFS.

Table 2
Parameters of the 2D geometries based on the CCFS packing.

2D layer	Unit	I	II	III	IV
D_Packing	mm	28.6	35.7	42.9	50
D_Reactor	mm	35.7	42.9	50	57.1
Total grid		64,000	76,800	89,600	102,400

Reactor height = 229 [mm]; packing height = 85.7 [mm]; gap width = 3.57 [mm]; packing channel diameter = 7.14 [mm]; channels diagonal angle = alternating 45, −45.

It is noted that the simulated, single-phase hydrodynamics might differ from the multiphase hydrodynamics inside the real reactor. We are currently extending the simulation code to two-phase flow. Nevertheless, the single-phase results can provide guidelines for packing optimization and more accurate two-phase flow simulations and experiments.

Isopar-M (liquid) with a kinematic viscosity of 3.8×10^{-6} (m^2/s) was considered to flow inside the packing. The Reynolds number equals 140 (based on liquid inlet velocity and reactor diameter).

3.2. Results and discussion

Fig. 11 shows the liquid streamlines in the different CCFS layers for single-phase (liquid) flow. The flow in the packing is inhomogeneous and in some channels the liquid remains stagnant. This malfunctioning of the packing can lead to drastic reduction in the catalyst efficiency. Furthermore, it can reduce the convective heat transfer in the packing element and increase the possibility of hot spot formation in the catalytic bed.

Fig. 12 shows the distribution of the *x*-component of the fluid velocity inside four different simulated 2D layers. From this figure the velocity vectors in the channels as well as in the gap regions can be observed. The *x*-component of the fluid velocity is the main source of radial heat transfer inside the packing element. Comparing the velocity distributions in different layers shows that the stagnant zones are more pronounced in the off-central layers of the CCFS packing, for which the layer width-to-height ratio is low. An inhomogeneous flow field implies inhomogeneous and poorer heat transport inside the packing. This problem might be reduced by decreasing the height of the stacked packing elements in order to promote mixing between them.

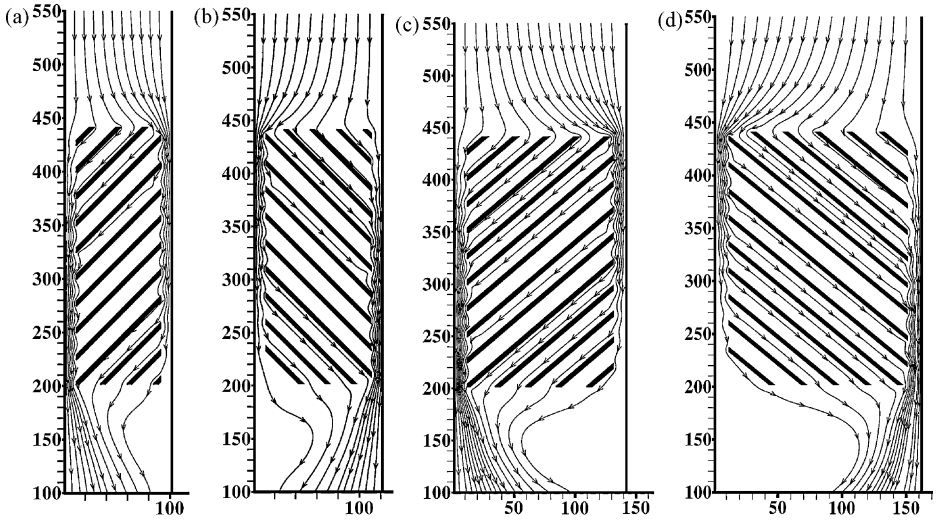

Fig. 11. Streamlines in different layers (a) layer I; (b) layer II; (c) layer III; (d) layer IV. The coordinates are scaled in lattices units, where 160 units correspond to the diameter of the central reactor layer.

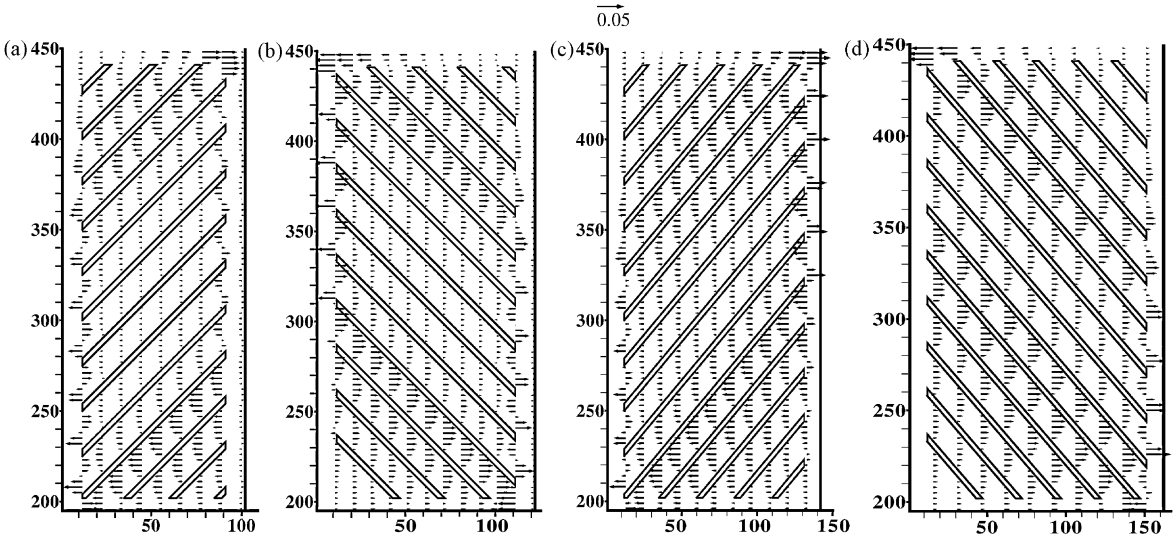

Fig. 12. *x*-Component of velocity vectors in different CCFS layers: (a) layer I; (b) layer II; (c) layer III; (d) layer IV. The coordinates are scaled in lattices units, where 160 units correspond to the diameter of the central reactor layer. The velocities are scaled based on the reference vector in the top middle of the figure.

The 2D velocity fields shown in Fig. 12 are based on simulations of individual layers, without considering the interactions between them. However, in reality, fluid exiting the diagonal channels, hits the reactor wall, changes direction and moves into the adjacent layers. This interaction between layers promotes the flow to pass through different layers of the packing element. Flow may also bypass the packing following a path in the gap region. The relative importance of these different possible flow paths depends on the gap- and channel-size as well as on the flow rate and pressure drop over the packing. Good reaction efficiency depends on homogeneous heat and flow distribution inside the packing which is achievable by optimizing the before mentioned parameters.

4. Conclusions

CFS packings perform much better in terms of overall heat transfer than the investigated randomly packed bed, foam packing, and the knitted wire packing in tubular reactors. This is largely the consequence of the presence of directed convective transport of the fluid flow through the channel geometry. Periodic redistribution of the liquid by alternating the packing orientation has a positive effect on the overall heat transfer. A large gap size between the packing structure and the cooling wall is shown to be beneficial for the overall heat transfer at large superficial gas velocities. At low superficial gas velocities the effect of different gap sizes on the overall heat transfer is negligible. A general 2D heat transport model, based on pseudo-homogeneous plug flow, is found inadequate to describe the radial temperature profile inside the tube. The deviations between model and experimental results occur because the model assumes radial symmetry, and does not take direction oriented transport of heat into account. Numerical experiments are performed to investigate the fluid flow inside the packing in detail. The geometry is defined as sheets separating layers of diagonal channels. For simplicity we assume no fluid exchange between different layers and we approximate the flow in the individual layers as 2D. The simulated velocity distribution inside the packing is highly inhomogeneous, showing regions of almost zero flow. These inhomogeneities, which can strongly impact reactor efficiency, are shown to depend on geometrical parameters, such as the packing width-to-height ratio. Currently, we are working towards full 3D simulations. These will enable us to study more complicated geometries like the OCFS packing or an array of packings with alternating orientation.

List of symbols

a_v	packing surface per volume (m^{-1})
C_p	specific heat ($J\,kg^{-1}\,K^{-1}$)
d_h	hydraulic diameter (m)
$\vec{e}_i$	velocity component in the lattice (l*u*/l*t*)
f_i	distribution function in direction $\vec{e}_i$
f_i^{eq}	equilibrium distribution function
r	radial coordinate (m)
R	tube radius (m)
t	time (s)
T	temperature (K)
u	fluid velocity ($m\,s^{-1}$)
U_{ov}	overall heat transfer coefficient ($W\,m^{-2}\,K^{-1}$)
z	axial coordinate (m)

Greek symbols

α_w	wall heat transfer coefficient ($W\,m^{-2}\,K^{-1}$)
ε	porosity
λ	heat conduction coefficient ($W\,m^{-1}\,K^{-1}$)
ρ	density ($kg\,m^{-3}$)

Acknowledgement

This research is supported by the Dutch Technology Foundation STW, the Applied Science Division of NWO and the Technology Program of the Ministry of Economic Affairs of the Netherlands. The authors would like to thank Claudia Cabral for carrying out part of the experimental work.

References

[1] A. Cybulski, J.A. Moulijn (Eds.), Structured Catalysts and Reactors, 2nd ed., CRC Taylor & Francis, Boca Raton, 2006.
[2] F. Kapteijn, J.J. Heiszwolf, T.A. Nijhuis, J.A. Moulijn, CATTECH 3 (1999) 24–41.
[3] R.M. de Deugd, R.B. Chougule, M.T. Kreutzer, F.M. Meeuse, J. Grievink, F. Kapteijn, J.A. Moulijn, Chem. Eng. Sci. 58 (2003) 583–591.
[4] R.M. de Deugd, F. Kapteijn, J.A. Moulijn, Top. Catal. 26 (1–4) (2003) 29–39.
[5] K. Pangarkar, T.J. Schildhauer, J.R. van Ommen, J. Nijenhuis, J.A. Moulijn, F. Kapteijn, Catal. Today 147 (2009) S2–S9.
[6] K. Pangarkar, T.J. Schildhauer, J.R. van Ommen, J. Nijenhuis, F. Kapteijn, J.A. Moulijn, Ind. Eng. Chem. Res. 47 (2008) 3720–3751.
[7] http://www.sulzerchemtech.com.
[8] K. Pangarkar, T.J. Schildhauer, J.R. van Ommen, J. Nijenhuis, F. Kapteijn, J.A. Moulijn, Chem. Eng. Sci., in preparation.
[9] C. von Scala, M. Wehrli, G. Gaiser, Chem. Eng. Sci. 54 (1999) 1375–1381.
[10] T.J. Schildhauer, E. Newson, A. Wokaun, Chem. Eng. Process. 48 (2009) 321–328.
[11] S. Succi, The Lattice Boltzmann Equation for Fluid Dynamics and Beyond, Clarendon Press, Oxford, 2001.
[12] J.P.L. Bhatnagar, E.P. Gross, M. Krook, Phys. Rev. 94 (1954) 511.